JOURNAL OF GUIDANCE, CONTROL, AND DYNAMICS
Vol. 28, No. 2, March–April 2005

Libration Control of Electrodynamic Tethers in Inclined Orbit

J. Peláez*
Technical University of Madrid, E-28040 Madrid, Spain
and
E. C. Lorenzini†
Harvard-Smithsonian Center for Astrophysics, Cambridge, Massachusetts 02138

Any electrodynamic tether working in an inclined orbit is affected by a dynamic instability generated by the continuos pumping of energy from electromagnetic forces into the tether attitude motion. To overcome the difficulties associated with this instability, two control schemes have been analyzed. In both cases the background strategy is the same: we add appropriate forces to the system with the aim of converting an unstable periodic orbit of the governing equations into an asymptotically stable one. The idea is to take such a stabilized periodic orbit as the starting point for the operation of the electrodynamic tether. In the first case, the unstable periodic orbit is taken as a reference orbit. In the second one, we use a delay feedback control scheme that has been used successfully in problems with one degree of freedom. To obtain results with broad validity, some simplifying assumptions have been introduced in the analysis. Thus, we assume a rigid tether with two end masses orbiting along a circular, inclined orbit. We also assume a constant tether current that does not depend on the attitude and orbital position of the tether, and the Earth's magnetic field is modeled as a dipole aligned with the Earth's rotation axis.

Nomenclature

a	=	radius of the center of mass circular orbit, km
$\boldsymbol{B}$	=	Earth magnetic field
$\mathcal{E}$	=	nondimensional total energy, defined in Eq. (17)
E_m	=	motional electric field, V/m, defined in Eq. (7)
f_e	=	electrodynamic torque factor, defined in Eq. (9)
h_1, h_2	=	auxiliary functions
I_m	=	tether current averaged over the total length, A, defined in Eq. (9)
$I(s)$	=	current distribution along the tether, A
i	=	orbital inclination, deg
k, k_1, k_2	=	control parameters
k^*	=	critical value of k
L	=	tether length, km
$\mathcal{L}$	=	Lagrangian function, J
m	=	tether mass, kg
m_B	=	mass of the end mass, kg
O	=	center of mass; origin on the orbital frame
Q_θ, Q_φ	=	generalized forces
$\tilde{Q}_\theta, \tilde{Q}_\varphi$	=	generalized forces
R	=	distance to the Earth center of mass, m
$\boldsymbol{R}$	=	position vector in the inertial frame, m
s	=	distance from the orbiter end O, m
T	=	kinetic energy of the system, J
$\mathcal{T}$	=	nondimensional kinetic energy of the system, defined in Eq. (16)
t	=	time, s
$\boldsymbol{u}$	=	unit vector along the tether, defined in Eq. (1)
$\boldsymbol{u}_m$	=	unit vector of the magnetic dipole
$\boldsymbol{u}_R$	=	unit vector in the radial direction [see Eq. (5)]
V	=	gravitational potential energy, J
$\mathcal{V}_0, \mathcal{V}_1$	=	nondimensional potential energies
$\boldsymbol{v}_s$	=	orbital velocity of the center of mass, m/s
$\boldsymbol{\gamma}^O$	=	acceleration of the center of mass, m/s^2
ε	=	electrodynamic parameter, defined in Eq. (15)
η_1, η_2	=	perturbation of the initial conditions, defined in Eqs. (24) and (25)
θ	=	tether in-plane angle, rad
θ_p, φ_p	=	basic periodic solution, rad
λ	=	eigenvalues of the monodromy matrix
μ	=	Earth's gravitational constant, km^3/s^2
μ_m	=	magnetic moment of the Earth's dipole, T · km^3
ν	=	true anomaly of the orbit of O, rad
ν_0	=	initial true anomaly, rad
φ	=	tether out-of-plane angle, rad
$\boldsymbol{\Omega}$	=	angular velocity of the orbital frame, s^{-1}
ω	=	angular frequency of the orbit, s^{-1}
$(\dot{\star})$	=	d$(\star)$/dν

Presented as AAS Paper 2003-214 at the AAS/AIAA 13th Space Flight Mechanics Meeting, Ponce, PR, 9–13 February 2003; received 21 November 2003; revision received 26 July 2004; accepted for publication 2 September 2004.

*Associate Professor, Escuela Técnica Superior de Ingenieros Aeronáuticos, Pl. Cardenal Cisneros 3; j.pelaez@upm.es. Member AIAA.

†Staff Scientist and Head, Special Projects Group, Radio and Geoastronomy Division, 60 Garden Street, MS-80; elorenzini@cfa.harvard.edu. Senior Member AIAA.

Introduction

RECENTLY, a challenging research subject has been arisen in the field of nonlinear dynamical system: the control of chaos, that is, the possibility of bringing order into chaos. Some investigations have been undertaken using control schemes with and without feedback. It seems that feedback schemes require comparatively small perturbations (see Ref. 1) to acquire control on the system.

Pyragas in Ref. 2 proposed a feedback control scheme designed to synchronize the current state of a system and a time-delayed version of itself. Taking this delayed time as the period of an unstable periodic orbit, such a control scheme can be used to stabilize the orbit. This method of control is usually named time-delayed autosynchronization or TDAS. Two important advantages of this method are related with the feedback used: it does not requires rapid switching or sampling, nor does it require a reference signal corresponding to the desired orbit. This technique has been improved in Refs. 3 and 4 using a more elaborated feedback: the extended time-delayed autosynchronization or ETDAS, where TDAS appears as a limiting case.

The central idea of these methods is to take advantage of the unstable periodic orbits, which usually appear embedded in chaotic attractors, that is, most of the research efforts were devoted to the control of chaotic behavior in low-dimensional dynamical systems. Such orbits can be controlled with small perturbation forces that decrease when time goes on because the system approaches the stabilized periodic orbit where they vanish. The instabilities considered are caused by various sources depending on the cases analyzed.

Control schemes using delayed feedback have been utilized in orbital and attitude dynamics of spacecrafts. One example of this kind of analysis can be found in Ref. 5 for a system with one degree of freedom. In that paper, a TDAS control law is used to stabilize the libration of a gravity-gradient satellite in an elliptical orbit. The libration of this kind of satellites exhibits a self-excited dynamics that is strongly chaotic in some regions of the parameter space.

Basically, an electrodynamic tether is made of a thin conductive wire. When flying in circular orbit, the inert tether, that is, the tether with zero current, has a stable equilibrium position on the local vertical. However, this gravity-gradient stabilized equilibrium position disappears when the current begins to flow in the wire. Instead of equilibrium positions, the governing equations exhibit periodic solutions with the period of the circular orbit followed by the system center of mass. In the absence of damping or control, these periodic orbits are unstable, and the dynamic instability involved increases with the tether current. Consequently, it is quite natural to investigate the possibility of stabilizing such periodic orbits using the techniques just mentioned that have been specially designed to stabilize chaotic periodic orbits.

The underlying instability has been studied in previous analysis with different dynamic models.[6–12] They show that the instability source which drives any electrodynamic tether unstable is a nonlinear resonance mechanism that pumps energy continually into the system. Eventually, the attitude motion of the tether relative to the orbital frame becomes unstable after several orbits. In those papers the tether current was assumed constant along the orbit and, in particular, independent of the actual tether position. This assumption, which we also adopt in this paper, permits one to obtain results with broad validity that can be applied to any kind of electrodynamic tether regardless of the particular device used to collect electrons from the surrounding plasma.

To lighten the analysis, we introduce some simplifying assumptions. Thus, the Earth's magnetic field is modeled as a dipole aligned with the Earth's rotation axis, and we assume a rigid tether with two end masses orbiting along a circular and inclined orbit. Thus, the analysis does not include the response of the tether lateral dynamics, which is also affected by the instability. However, the control of the librations is a necessary condition to the reliable operation of the tether; unfortunately, it is not sufficient. Because the coupling between librations and lateral modes is complex as a result of the electrodynamic forces (see Ref. 13 for a linear approximation), a further analysis would be required to asses the behavior of the lateral modes.

In this paper we carry out two different analyses about the stability properties of the periodic solutions that characterize electrodynamic tethers in inclined orbits. In the first analysis a particular periodic solution is taken as the reference solution. We show that this solution, which is unstable without damping or control, becomes asymptotically stable when the system is controlled using the scheme proposed in this paper. To obtain the families of periodic solutions that appear in the analysis and their stability properties, we use a numeric algorithm, which is described in Ref. 14.

In the second analysis we carry out a brief introduction on the application of the delay feedback control scheme to the rigid electrodynamic tether. We follow closely the analysis of Ref. 5 trying to extend it to system with two degrees of freedom.

In both cases the background strategy is the same: we add appropriate forces to the system with the aim of converting an unstable periodic orbit of the governing equations into an asymptotically stable one. The idea is to take such a stabilized periodic orbit as the starting point for the operation of the electrodynamic tether. Notice that electrodynamic tethers used to generate thrust are most attractive when operated over long periods of time. From this point of view, the stable character of the periodic orbit should be considered as an important system requirement.

On the other hand, to control the tether the appropriate forces must be introduced in the system with the help of some device. This poses an important problem facing the operation of the electrodynamic tether: which kind of device should be used to apply these forces on the system? For the moment, we disregard that problem, assuming that the appropriate forces are available. However, we point here to a possible solution: to use a movable boom to act on the tether attaching point to introduce such forces.

Finally, the mechanism that destabilizes the electrodynamic tether in inclined orbits is different from others considered in the literature, which were associated with chaotic motions without a continuous increase of the total energy of the system. Here, the energy ends up increasing continually because of the forcing terms of the governing equations associated with the electrodynamic forces.

Description of the Basic Tether Model

The tether is considered as a thin rigid rod with mass m and length L. A point mass m_B is attached to the higher end of the tether. The orbiter O is at the lower end. We assume the mass of the orbiter to be very large compared with the remaining masses of the system, and we neglect its orbital decay. As a consequence, the orbiter is tracing a circular orbit of radius a and inclination i, with an angular rate $\omega = \sqrt{(\mu/a^3)}$.

We used two right oriented reference frames:

1) The first is the inertial geocentric frame $Ex_1y_1z_1$: the origin at the center of mass of the Earth E, the Ex_1 axis pointing to the first Aries point, and the Ez_1 axis aligned with the Earth's rotation axis.

2) The second is the orbital frame $Oxyz$, with origin O at the orbiter, the Ox axis along the local vertical pointing to zenith, the Oz axis directed along the velocity vector, and the Oy axis normal to the orbital plane (Fig. 1). The angular velocity of the orbital frame $\boldsymbol{\Omega}$ and the acceleration of its origin $\boldsymbol{\gamma}^O$ take the values

$$\boldsymbol{\Omega} = -\omega \boldsymbol{j}, \qquad \boldsymbol{\gamma}^O = -\omega^2 a \boldsymbol{i}$$

The position of the tether in the orbital frame and its unit vector $\boldsymbol{u}$

$$\boldsymbol{u} = (\cos\varphi\cos\theta, -\sin\varphi, \cos\varphi\sin\theta) \tag{1}$$

are defined by the in-plane and the out-of-plane angles: θ and φ, respectively. These angles will be taken as generalized coordinates to study the dynamics of the system. On the other hand, because the system is subject to ideal constraints the methods of analytical dynamics can be used to derive the equations governing its dynamics. For this purpose, the expressions of the kinetic energy and the virtual work of the applied forces will be computed.

In the motion relative to the inertial frame, the kinetic energy is a function of the generalized coordinates and velocities given by

$$T = \tfrac{1}{2}M\omega^2a^2 + \tfrac{1}{2}\left(\tfrac{1}{3}m + m_B\right)L^2\omega^2[\dot{\varphi}^2 + (1+\dot{\theta})^2\cos^2\varphi] \tag{2}$$

M is the total mass of the system ($M \gg m_B, m$), and the first term of the right-hand side is a constant value for a circular unperturbed orbit that does not play any role in the analysis.

The gravitational forces derive from a potential function. The virtual work of the electrodynamic forces should be determined from the expression of their power because the system is scleronomic.

Gravitational Forces

Let $\boldsymbol{r}$ be the position vector in the orbital frame of a differential mass dm of the system. We consider the Earth with spherical symmetry. As a consequence, the orbital plane will remain steady in the

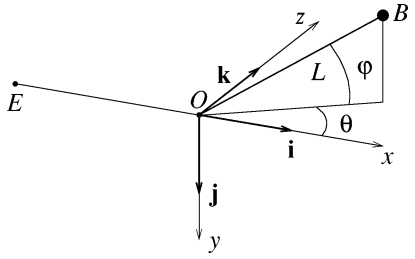

Fig. 1 Orbital frame and tether position.

inertial geocentric frame $Ex_1y_1z_1$. Let dm be a differential mass at a distance $R = \|a\boldsymbol{i} + \boldsymbol{r}\|$ from the Earth's center. Its gravitational potential is

$$V^{dm} = -\mu dm/R$$

This expression will be developed as a Taylor series up to terms of order $(L/a)^2$ about the origin O of the orbital frame ($\boldsymbol{r} = 0$) to obtain

$$V^{dm} = -(\mu/a)\left[1 - (\boldsymbol{r}\cdot\boldsymbol{i})/a + \tfrac{3}{2}(\|\boldsymbol{r}\cdot\boldsymbol{i}\|^2/a^2) - \tfrac{1}{2}(\|\boldsymbol{r}\|^2/a^2)\right]dm \tag{3}$$

For the whole system, the potential of the gravitational forces is obtained in two steps: 1) the vector $\boldsymbol{r}$ in Eq. (3) is written as a function of the generalized coordinates and 2) the expression (3) is integrated over the whole system to yield

$$V = -\tfrac{1}{2}\left(m_B + \tfrac{1}{3}m\right)\omega^2 L^2 \cdot 3\cos^2\varphi\cos^2\theta \tag{4}$$

where constant terms have been removed.

Electrodynamic Forces

The Earth magnetic field $\boldsymbol{B}$ is modeled by means of a dipole with origin at the Earth's center of mass and whose axis is defined by the unit vector $\boldsymbol{u}_m$. Let $\boldsymbol{R} = R\boldsymbol{u}_R$ be the position vector of a given point P; then the field $\boldsymbol{B}$ in P, is

$$\boldsymbol{B}(\boldsymbol{R}) = \left(\mu_m \big/ R^3\right)[\boldsymbol{u}_m - 3(\boldsymbol{u}_m\cdot\boldsymbol{u}_R)\boldsymbol{u}_R] \tag{5}$$

In a tilted dipole model the unit vector $\boldsymbol{u}_m$ would rotate around the Earth's spin axis. In this paper, for simplicity we neglect the tilt, which is not essential in explaining the instability mechanism of the electrodynamic tethers as long as the orbits are inclined.

We assume the tether length L to be much smaller than the characteristic length of variation of the Earth's magnetic field. Thus, the value of $\boldsymbol{B}$ at any tether point will be equal to the value of $\boldsymbol{B}$ at the origin O ($R\boldsymbol{u}_R \approx a\boldsymbol{i}$). In such a case, the unit vector $\boldsymbol{u}_m$ becomes (see Refs. 6 and 7 for details)

$$\boldsymbol{u}_m = \sin i\sin\nu\,\boldsymbol{i} - \cos i\,\boldsymbol{j} + \sin i\cos\nu\boldsymbol{k}$$

Along the orbit, the dipole model provides the following components, in the orbital frame, of the magnetic field $\boldsymbol{B} = B_x\boldsymbol{i} + B_y\boldsymbol{j} + B_z\boldsymbol{k}$:

$$B_x = -\left(2\mu_m \big/ a^3\right)\sin i\sin\nu, \qquad B_y = -\left(\mu_m \big/ a^3\right)\cos i$$

$$B_z = +\left(\mu_m \big/ a^3\right)\sin i\cos\nu \tag{6}$$

For an orbital velocity $\boldsymbol{v}_s$, the geomagnetic field $\boldsymbol{B}$ induces, in the tether reference frame, a motional electric field

$$E_m = \boldsymbol{u}\cdot(\boldsymbol{v}_s \times \boldsymbol{B}) \tag{7}$$

which drives an electric current $I(s)$ along the tether, provided that a good, steady electric contact is achieved with the ionospheric plasma for both electron collection and emission. The relationship between E_m and $I(s)$ depends on the configuration and regime of the electrodynamic tether.

Next, we will obtain the generalized forces associated with the electrodynamic terms. Let ds be the differential length of a tether element at a distance s from the point O. Its position vector in the inertial frame $Ex_1y_1z_1$ is $\boldsymbol{x}^{ds} = a\boldsymbol{i} + s\boldsymbol{u}$. If the tether current is $I(s)$, the force acting on this element is

$$\boldsymbol{F}_B^{ds} = I(s)ds\,\boldsymbol{u}\times\boldsymbol{B} \tag{8}$$

The generalized forces produced by these magnetic forces are given by

$$Q_\theta = \int_0^L \boldsymbol{F}_B^{ds}\cdot\frac{\partial\boldsymbol{x}^{ds}}{\partial\theta} = \int_0^L sI(s)ds(\boldsymbol{u}\times\boldsymbol{B})\cdot\frac{\partial\boldsymbol{u}}{\partial\theta}$$

$$Q_\varphi = \int_0^L \boldsymbol{F}_B^{ds}\cdot\frac{\partial\boldsymbol{x}^{ds}}{\partial\varphi} = \int_0^L sI(s)ds(\boldsymbol{u}\times\boldsymbol{B})\cdot\frac{\partial\boldsymbol{u}}{\partial\varphi}$$

Introducing into these expressions Eqs. (1) and (6) and integrating over the whole tether length, the generalized forces result in

$$Q_\theta = -f_e I_m L^2\left(\mu_m \big/ a^3\right)\cos\varphi$$
$$\times[\sin i\sin\varphi(2\sin\nu\cos\theta - \cos\nu\sin\theta) + \cos i\cos\varphi]$$

$$Q_\varphi = f_e I_m L^2\left(\mu_m \big/ a^3\right)\sin i(2\sin\nu\sin\theta + \cos\nu\cos\theta)$$

where the constant f_e and the average electric current I_m are defined by the following integrals:

$$I_m = \frac{1}{L}\int_0^L I(s)ds, \qquad f_e I_m L^2 = \int_0^L sI(s)ds \tag{9}$$

Notice that $f_e = \frac{1}{2}$ when the tether current is uniform along the tether. However, the distribution of current along the tether $I(s)$ depends on the tether configuration and the regime of operation. There are two basic configurations: 1) the insulated tether, with current collection and emission only at end masses; and 2) the bare tether, with current collection along its anodic portion. An electrodynamic tether has two basic operation regimes: the thruster mode, with $I_m < 0$, and the generator (deboost) mode, with $I_m > 0$. In the generator mode the tether collects electrons from the ionosphere at its upper end. These electrons are then ejected back into the ionosphere by the cathodic contactor at the lower end; thus, the conventional current flows from the lower to the higher end of the tether. In the thruster mode the current is forced to flow in the opposite direction by means of a power supply that bias the tether positively with respect to the ambient plasma. The analysis of papers[6,7,9,10] can be applied to both tether configurations and both operation regimes.

Uncontrolled System

In this section we derive the system governing equations without control. In such a case, the only forces that must be considered are the gravitational, inertial, and electrodynamic forces. Moreover, we will assume constant the value of the parameter ε, defined in Eq. (15). Notice that to achieve this condition the tether current must be kept constant along the orbit (see later on).

Governing Equations

A Lagrangian function $\mathcal{L} = T - V$, which does not include the electrodynamic forces, can be defined for the system as follows:

$$\mathcal{L} = \tfrac{1}{2}\omega^2 L^2\left(m_B + \tfrac{1}{3}m\right)\{\dot\varphi^2 + \cos^2\varphi[3\cos^2\theta + (1+\dot\theta)^2]\} \tag{10}$$

and the Lagrange equations governing the system dynamics take the form:

$$\frac{\mathrm{d}}{\mathrm{d}\nu}\left(\frac{\partial\mathcal{L}}{\partial\dot\theta}\right) - \frac{\partial\mathcal{L}}{\partial\theta} = Q_\theta, \qquad \frac{\mathrm{d}}{\mathrm{d}\nu}\left(\frac{\partial\mathcal{L}}{\partial\dot\varphi}\right) - \frac{\partial\mathcal{L}}{\partial\varphi} = Q_\varphi$$

After replacing the generalized forces on the right-hand sides, the following system of equations is obtained:

$$\ddot\theta = 2(1+\dot\theta)\dot\varphi\tan\varphi - \tfrac{3}{2}\sin 2\theta - \varepsilon[\sin i\tan\varphi h_1(z,\theta) + \cos i] \tag{11}$$

$$\ddot\varphi = -\tfrac{1}{2}\sin 2\varphi[(1+\dot\theta)^2 + 3\cos^2\theta] + \varepsilon\sin i\,h_2(z,\theta) \tag{12}$$

$$\dot z = 1 \tag{13}$$

where h_1 and h_2 are auxiliary functions defined as follows:

$$h_1(z,\theta) = 2\sin z\cos\theta - \cos z\sin\theta$$

$$h_2(z,\theta) = 2\sin z\sin\theta + \cos z\cos\theta$$

In these equations, and along the paper, the dot means derivation with respect to the true anomaly ν, measured from the lines of nodes $\nu = \nu_0 + \omega t$. The variable z has been introduced to make the system of differential equations autonomous. It is defined in one period $[z_0, z_0 + 2\pi]$, and it coincides with the true anomaly ν but for a constant.

The tether current is on at the initial time ($t = 0$), and Eqs. (11–13) must be integrated starting from the appropriate initial conditions

$$\text{at} \qquad \nu = \nu_0(t=0), \qquad \theta = \theta_0$$

$$\varphi = \varphi_0, \qquad \dot\theta = \dot\theta_0, \qquad \dot\varphi = \dot\varphi_0 \tag{14}$$

The main effect of the electrodynamic forces is included in the nondimensional parameter ε:

$$\varepsilon = \frac{3 f_e I_m}{m + 3m_B} \cdot \frac{\mu_m}{\mu} \tag{15}$$

Therefore, there are only two free parameters, ε and i, in Eqs. (11–13), which govern the systems dynamics.

Energy Equation

The kinetic energy of the system in its motion relative to the orbital frame takes the following nondimensional form:

$$\mathcal{T} = \tfrac{1}{2}(\dot\varphi^2 + \dot\theta^2\cos^2\varphi) \tag{16}$$

The other terms of the Lagrangian function can be considered as 1) an ordinary potential V_0 and 2) a generalized potential V_1. They have the following nondimensional form:

$$\mathcal{V}_0 = \tfrac{1}{2}[4 - \cos^2\varphi(1 + 3\cos^2\theta)], \qquad \mathcal{V}_1 = -\dot\theta\cos^2\varphi$$

and from them the gravitational and inertial forces can be derived.

Note that the generalized forces derived from $\mathcal{V}_1$

$$\tilde Q_\theta = \frac{\mathrm{d}}{\mathrm{d}\nu}\left(\frac{\partial \mathcal{V}_1}{\partial \dot\theta}\right) - \frac{\partial \mathcal{V}_1}{\partial \theta}, \qquad \tilde Q_\varphi = \frac{\mathrm{d}}{\mathrm{d}\nu}\left(\frac{\partial \mathcal{V}_1}{\partial \dot\varphi}\right) - \frac{\partial \mathcal{V}_1}{\partial \varphi}$$

are gyroscopic, that is, they produce no power: $\dot\theta\tilde Q_\theta + \dot\varphi\tilde Q_\varphi = 0$.

By definition, the total energy of the system relative to the orbital reference frame takes the following nondimensional form:

$$\mathcal{E} = \mathcal{T} + \mathcal{V}_0 \tag{17}$$

and its evolution is governed by the energy equation, which takes the form

$$\frac{\mathrm{d}\mathcal{E}}{\mathrm{d}\nu} = \varepsilon\left\{\dot\varphi\sin i\, h_2(\nu,\theta) - \dot\theta\cos^2\varphi[\sin i\sin\varphi h_1(\nu,\theta) + \cos\varphi\cos i]\right\} \tag{18}$$

On the right-hand side of this equation, there is only one term giving the power produced by the electrodynamic forces.

Basic Periodic Solution

For the uncontrolled system, the dynamics is governed by Eqs. (11) and (12). The numerical integration of these equations, starting from the initial conditions (14), provides the time evolution of the tether position, which depends on the free parameters of the model: ε and i.

When $\varepsilon = 0$, the governing equations (12) and (13) exhibit steady solutions. In one of these singular points, the tether is aligned along the vertical ($\theta = \varphi = 0$), and this equilibrium position is stable.

When $\varepsilon \neq 0$, that is, when the current is flowing in the conductive tether, the steady solutions disappear. Instead of equilibrium positions the governing equations (11) and (12) exhibit periodic solutions with the orbital period (2π in nondimensional variables).

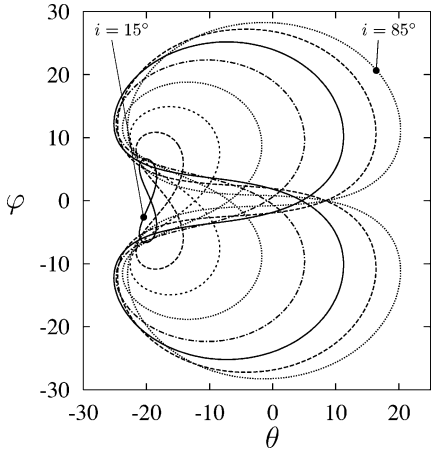

Fig. 2 Basic periodic solutions for $\varepsilon = 1.0$ and different values of i from $i = 15$ to 85 deg by 10-deg increments.

The basic periodic solutions depend on the two free parameters ε and i. Figures 2 and 3 show the form of these periodic solutions for different values of ε and i. Figure 2 shows the form of the basic periodic solution when $\varepsilon = 1.0$. Eight cases have been plotted corresponding to the following values of the orbital inclination: $i = 15$, 25, 35, 45, 55, 65, 75, and 85 deg. For small values of i, the periodic solution is an oscillation in φ with θ almost constant. For increasing values of i, the amplitudes of both angles grows noticeably.

Figure 3 shows the periodic solutions for the same values of the orbital inclination in two additional cases: $\varepsilon = 0.5$ and 1.5. Notice that when $\varepsilon = 0.5$, the amplitudes become small. (In fact they are smaller than $\approx$15 deg.) On the contrary, when $\varepsilon = 1.5$ the amplitudes become significant, and they reach values close to 90 deg. From these pictures, it is clear that the amplitudes of both oscillations growth monotonously with ε.

The stability properties of the basic periodic solution also depend on the two free parameters ε and i. It is a well-known fact that this periodic solution is unstable for all values of ε and i, when the system is not controlled or damped, which is the case that we study here (see, for example, Refs. 6, 7, 9, and 10). In the following sections we will consider the case in which the tether is controlled and this basic periodic solution will be taken as a reference orbit.

First Control Scheme

In the first control scheme we will use the following governing equations:

$$\ddot\theta - 2(1+\dot\theta)\dot\varphi\tan\varphi + \tfrac{3}{2}\sin 2\theta = -\varepsilon\cdot[\sin i\tan\varphi h_1(\nu,\theta) + \cos i] - k_1[\dot\theta(\nu) - \dot\theta_p(\nu)] \tag{19}$$

$$\ddot\varphi + \sin\varphi\cos\varphi\{(1+\dot\theta)^2 + 3\cos^2\theta\} = \varepsilon\sin i\cdot h_2(\nu,\theta) - k_2\{\dot\varphi(\nu) - \dot\varphi_p(\nu)\} \tag{20}$$

In the right-hand side of these controlled equations (19) and (20) appear $\theta_p(\nu)$, $\varphi_p(\nu)$, which represent the basic periodic solution of the noncontrolled system (11) and (12); $\theta = \theta_p(\nu,\varepsilon,i)$, and $\varphi = \varphi_p(\nu,\varepsilon,i)$ for given values of ε and i. Note that those unstable periodic solutions are also solutions of these new equations (19) and (20) for nonvanishing values of the control parameters, that is, when $(k_1, k_2) \neq (0, 0)$ because the control terms vanish when the system follows such 2π-periodic solutions.

To simplify the analysis, we consider the case in which both parameters k_1 and k_2 take the same value: $k_1 = k_2 = k$. In such a case the governing equations involve three free parameters, and the stability properties can be described as functions of k for given values of i and ε.

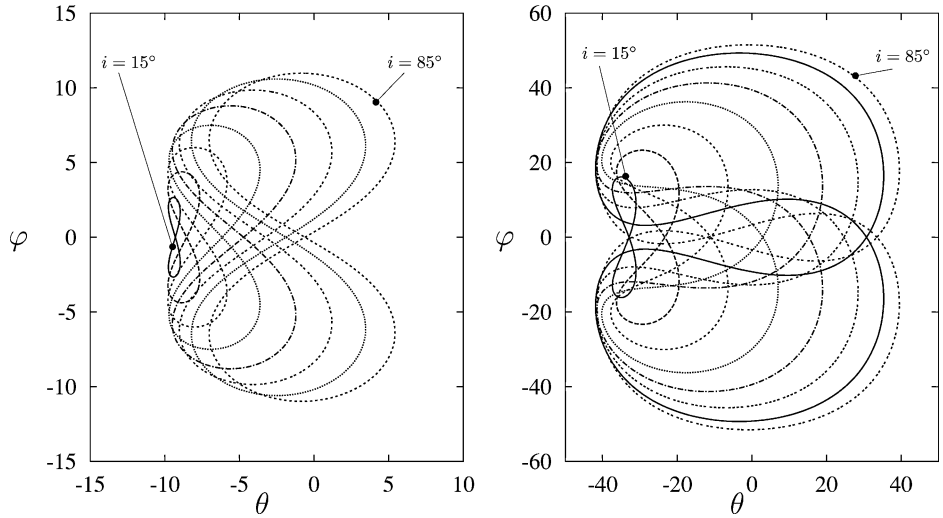

Fig. 3 Basic periodic solutions for a) $\varepsilon = 0.5$ and b) $\varepsilon = 1.5$. The inclination i takes the same values as in Fig. 2.

Note that in this control scheme, we are taking the basic periodic solution as the reference orbit, and the control process will be organized around such a periodic orbit. Therefore, we will analyze first the stability properties of this simplified control scheme. Then we will use the results of this analysis to check the TDAS control scheme.

Stability Properties

For a numerical example, let us assume the values of i and ε, for example,

$$\varepsilon = 1.5, \qquad i = 40 \text{ deg} \tag{21}$$

The basic periodic solution of the noncontrolled system (11) and (12), which depends only on ε and i, can be readily obtained. It will also be a 2π-periodic solution of the system (19) and (20) for any value of the control parameter k. For the case we had just selected, the initial conditions (at $v_0 = 0$) that lead to the periodic orbit are

$$\theta_0 = 0.00268, \qquad \varphi_0 = 0.29677 \tag{22}$$

$$\dot{\theta}_0 = 0.12715, \qquad \dot{\varphi}_0 = -0.76264 \tag{23}$$

and the basic periodic solution is shown in Fig. 4. These values have been obtained with the help of the numeric algorithm described in.[14]

To obtain this curve, Eqs. (11) and (12) have been integrated, starting from the initial conditions (22) and (23) and for the values (21) of the free parameters. Because the orbit is also a periodic solution of the controlled system, it can be obtained by integrating Eqs. (19) and (20), starting from the same initial conditions (22) and (23) and with the same values of ε and i. However, in the second orbit the control parameter k is not zero (in particular we take $k = 0.25$ in this case). The agreement between both numerical solutions (one is given by the solid line and the other by the dots) is perfect, as it should be.

Thus, if the value of k is changed the basic periodic solution considered as orbit of Eqs. (19) and (20) does not change, but its stability properties do, and this is the most important point of the procedure.

The periodic solution shown in Fig. 4 is unstable as we show in the following. To confirm this unstable character, we integrate Eqs. (11) and (12) starting from the following initial conditions [the initial conditions (22) and (23) perturbed]:

$$\theta_0 = 0.00268 + \eta_1, \qquad \varphi_0 = 0.29677 + \eta_2 \tag{24}$$

$$\dot{\theta}_0 = 0.12715, \qquad \dot{\varphi}_0 = -0.76264 \tag{25}$$

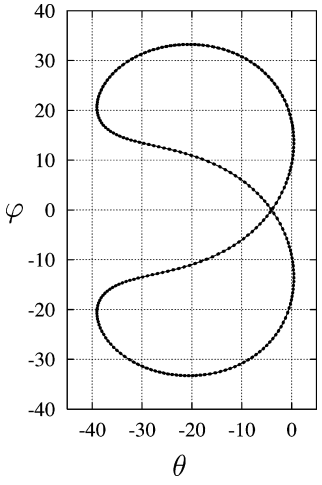

Fig. 4 Basic periodic solutions. Here $\varepsilon = 1.5$, and $i = 40$ deg ($k = 0$ and 0.25).

When $(\eta_1, \eta_2) \neq (0, 0)$, they lead to an orbit that is quite different from the periodic solution, even for values of η_1 and η_2 as small as $\eta_1 = 0.01$ and $\eta_2 = 0.01$. For these values, we should get an orbit of the uncontrolled Eqs. (11) and (12), which should remain close to the periodic orbit shown in Fig. 4. However, because of the unstable character of the basic periodic solution, when times increases the orbits will diverge.

Figure 5 shows the trajectory of the uncontrolled equations (11) and (12), which starts from the initial conditions (24) and (25), that is, almost on the periodic orbit.

However, Fig. 5 shows clearly the increasing separation between both orbits. In fact, after six orbital periods the new trajectory is very close to the transition from libration to rotation, that is, it is far away from the periodic orbit.

Figure 6a shows the evolution of the eigenvalues of the monodromy matrix of the periodic solution plotted in Fig. 4, when the parameter k takes increasing values starting from zero. For this particular case, the four eigenvalues of the monodromy matrix appear as two pairs of complex conjugate numbers. When $k = 0$ (uncontrolled system), one pair has modulus greater than one, and the periodic solution shown in Fig. 4 is unstable.

Figure 6b shows the moduli of the eigenvalues of the monodromy matrix as functions of k. It is clear that the moduli decrease when k increases. Thus, when k reaches a critical value $k^* \approx 0.1675$ the maximum modulus of the eigenvalues is exactly 1, and when $k > k^*$ all of the eigenvalues have moduli lower than 1. The critical value k^* is the boundary where the basic periodic solution changes from unstable to stable.

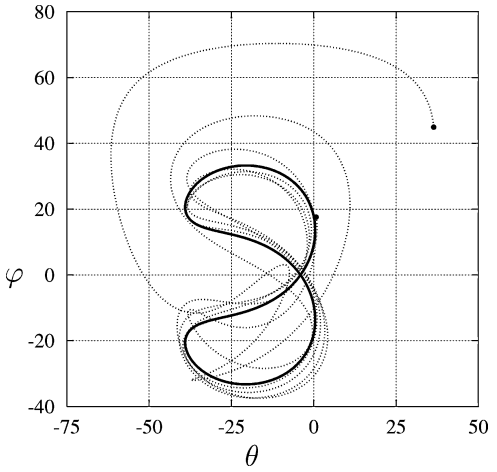

Fig. 5 Unstable behavior of the periodic solution in the case $\varepsilon = 1.5$, $i = 40$ deg. Six orbital periods.

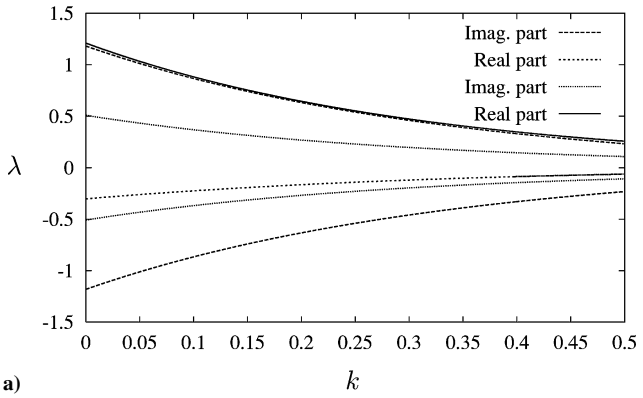

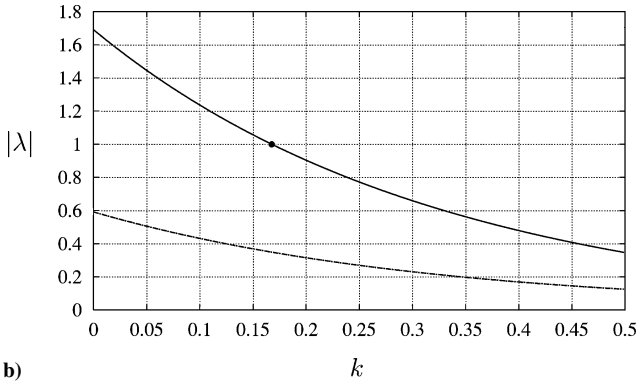

Fig. 6 Eigenvalues of the monodromy matrix and moduli vs k for $i = 40$ deg and $\varepsilon = 1.5$.

In summary, when $k < k^*$ the unstable character of the basic periodic solution does not change. However, when $k > k^*$ then the control law stabilizes the basic periodic solution, which becomes asymptotically stable because the eigenvalues of the monodromy matrix has moduli strictly lower than 1.

When $k < k^*$, the control law improves the stability properties of the system, but it does not change the unstable character of the basic periodic solution. To check this behavior, we take $k = 0.10$ (a value lower than $k^* \approx 0.1675$). Figure 7 shows the trajectory of the controlled equations (19) and (20), which starts from the initial conditions (24) and (25) in this case. Notice that the only difference between the cases shown in Figs. 5 and 7 is the value of the parameter k, which is zero in the first case and $k = 0.10$ in the second one.

When $k > k^*$, the control law changes the character of the basic periodic solution, which becomes asymptotically stable. To confirm this behavior, we take $k = 0.20$, a value greater than $k^* \approx 0.1675$.

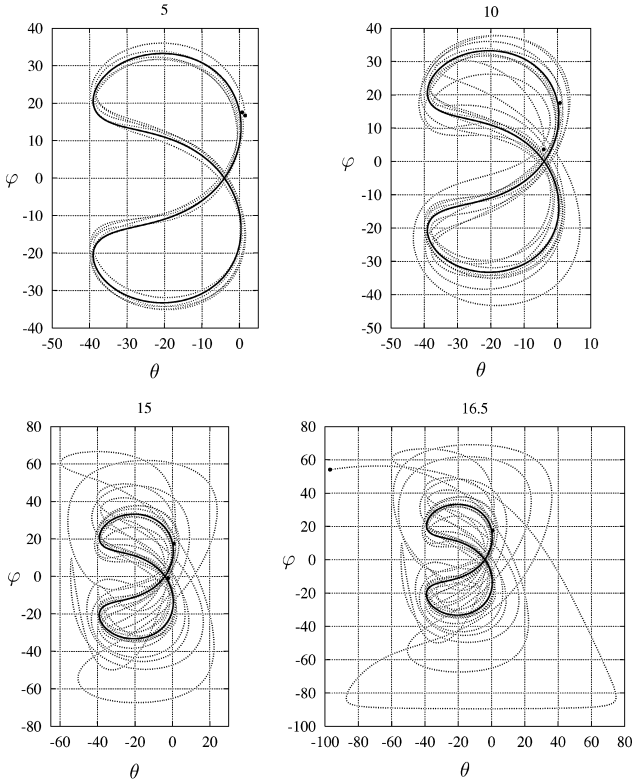

Fig. 7 In this run $k = 0.10 < k^*$. From top (left) to bottom (right): trajectory after 5, 10, 15, and 16.5 orbital periods.

Figure 8 shows the orbit resulting from numerical integration. Four different pictures are shown. The first picture depicts the trajectory during the first five orbital periods. The other pictures show the trajectory after 10, 15, and 20 orbital periods. Now, the trajectory remains close to the periodic orbit, and when time goes on both orbits are closer to one another.

Figure 9 shows $\triangle = |\boldsymbol{y}(\nu) - \boldsymbol{y}_p(\nu)|$, the difference between the trajectory and the basic periodic solution, as a function of the number of orbital periods (true anomaly). After 20 orbits this difference is almost half of its initial value, and after 40 orbits is, roughly, one-tenth. However, more important than the numerical values is the fact that the trend of this difference is clearly decreasing. After some number of orbits, the trajectory is so close to the basic periodic solution that is imposible to distinguish it.

The main conclusion of this analysis is that for these particular values of ε and i there is a critical value of the control parameter k^*, beyond which the basic periodic solution becomes asymptotically stable. The same qualitative behavior appears for different values of ε and i, as we will show in what follows.

Stability Domains

Let $|\lambda|_{\max}$ be the maximum modulus of the eigenvalues of the monodromy matrix of the basic periodic solution. The modulus is an involved function of the free parameters: $|\lambda|_{\max} = \Lambda(\varepsilon, i, k)$. The following step in the analysis is to keep the same value for the inclination $i = 40$ deg and to explore what happen when the parameter ε changes. Figure 10 shows the evolution of the eigenvalues of the monodromy matrix with the control parameter k, for the particular value of $\varepsilon = 1.0$.

From a qualitative point of view, there are no differences between this case ($\varepsilon = 1.0$) and the case shown in Fig. 6 ($\varepsilon = 1.5$). Like in the preceding case, there is also a critical value beyond which $|\lambda|_{\max} < 1$, and that implies the asymptotically stable character of the basic periodic solution.

The calculations made for several values of ε show essentially the same behavior. Moreover, changing the value of the inclination i does not change this qualitative behavior. As a consequence, there

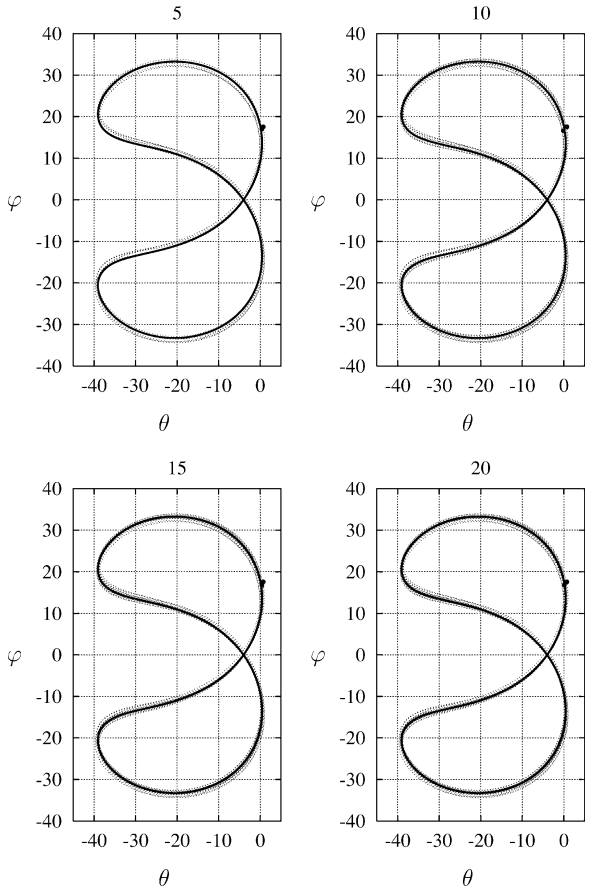

Fig. 8 Stabilization with $k = 0.2 > k^* \approx 0.16$. From top (left) to bottom (right): trajectory after 5, 10, 15, and 20 orbital periods.

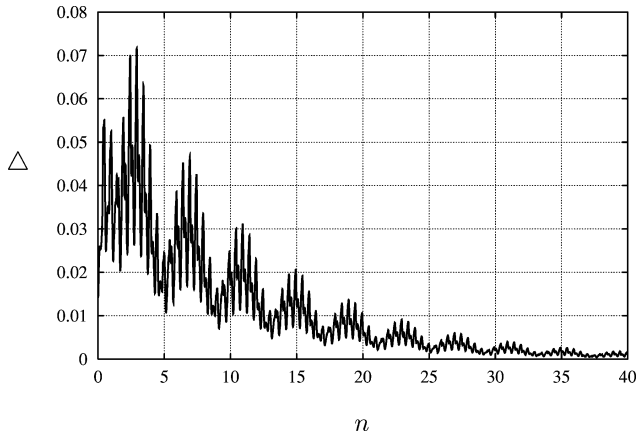

Fig. 9 Difference $\triangle = |y(\nu) - y_p(\nu)|$ vs the number of orbits n.

is a function that provides the stability boundary of the basic periodic solution. This function, which correspond to the condition $|\lambda|_{\max} = 1$,

$$\Lambda(\varepsilon, i, k) = 1 \Leftrightarrow k = k^*(\varepsilon, i) \tag{26}$$

has been numerically determined for some inclinations as we show in what follows.

Figure 11 shows this stability boundary in the plane (ε, k) when $i = 40$ deg. It corresponds to the curve $k = k^*(\varepsilon, i = 40 \text{ deg})$ obtained from Eq. (26) for this particular value of i. The curve divides the plane (ε, k) in two different regions: in one of them the basic periodic solution is unstable ($|\lambda|_{\max} > 1$), and in the other one is asymptotically stable ($|\lambda|_{\max} < 1$). On the boundary $|\lambda|_{\max} = 1$.

In fact, the stability boundary has two branches. The main branch, which is coming from the origin ($k = 0$, $\varepsilon = 0$), is the most significant; the secondary branch only appears for large values of ε, and it is caused by the existence of multiple solutions of the equations $|\lambda|_{\max} = 1$ beyond some critical value of ε.

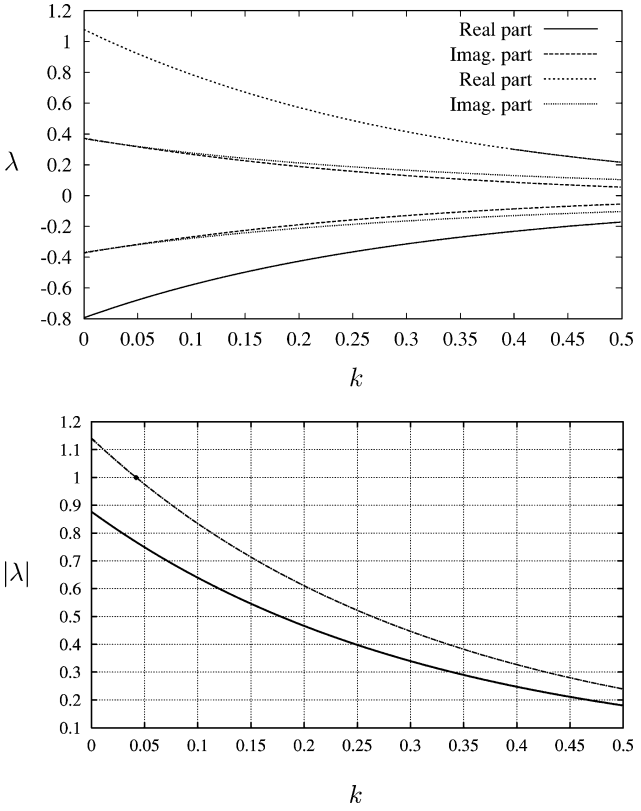

Fig. 10 Eigenvalues of the monodromy matrix and moduli vs k for $i = 40$ deg and $\varepsilon = 1.0$.

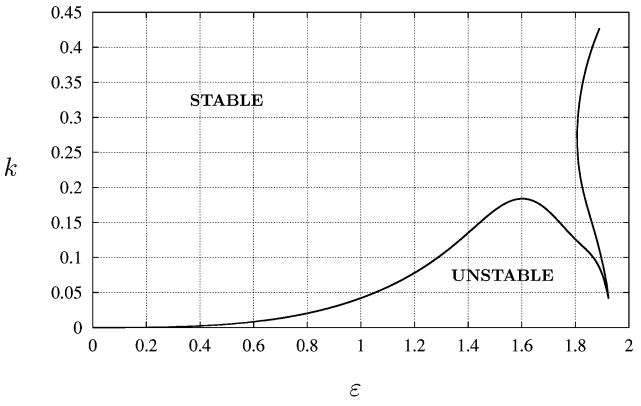

Fig. 11 Stability domain in the plane (ε, k) for $i = 40$ deg.

Figures 12 and 13 help in understanding the existence of the secondary branch of the stability boundary, in this particular case $i = 40$ deg. They show the eigenvalues of the monodromy matrix vs k for $\varepsilon = 1.7$ (one solution) and $\varepsilon = 1.82$ (three solutions), respectively. In the first case, Fig. 12, a pair of complex conjugate eigenvalues splits in two real eigenvalues beyond some value of k. However, there is only one root of the equation $|\lambda|_{\max} = 1$.

In the second case, Fig. 13, there are three roots of the equations $|\lambda|_{\max} = 1$, namely, k_1, k_2, and k_3. One of the two real eigenvalues has modulus larger than 1 in the interval $[k_2, k_3]$. The ends of this interval give the secondary branch of the stability boundary.

The numerical analysis has been carried out for $i = 40$ deg and for other values of the inclination i. The results obtained are summarized in Fig. 14, which shows the stability boundary in the plane (ε, k) for $i = 20$, 25, 30, 35, and 40 deg.

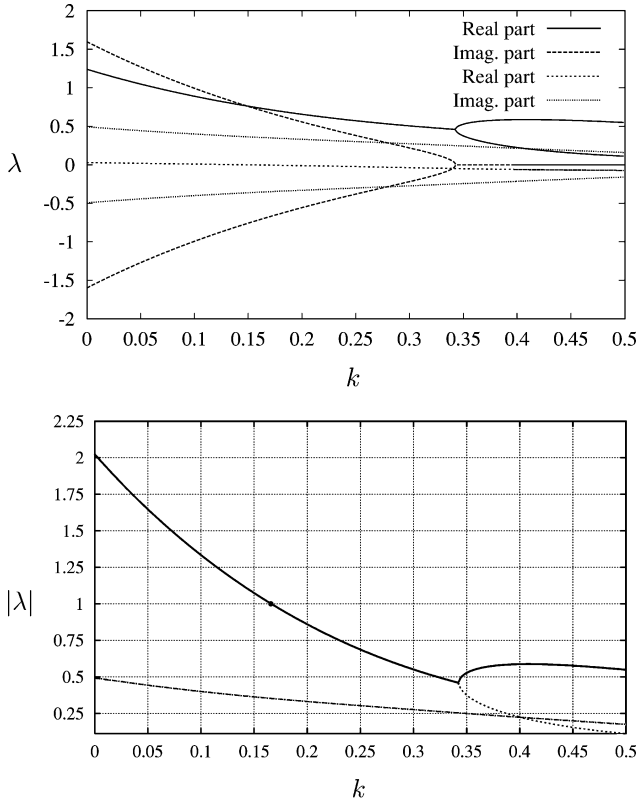

Fig. 12 Eigenvalues of the monodromy matrix and moduli vs k for $i = 40$ deg and $\varepsilon = 1.7$.

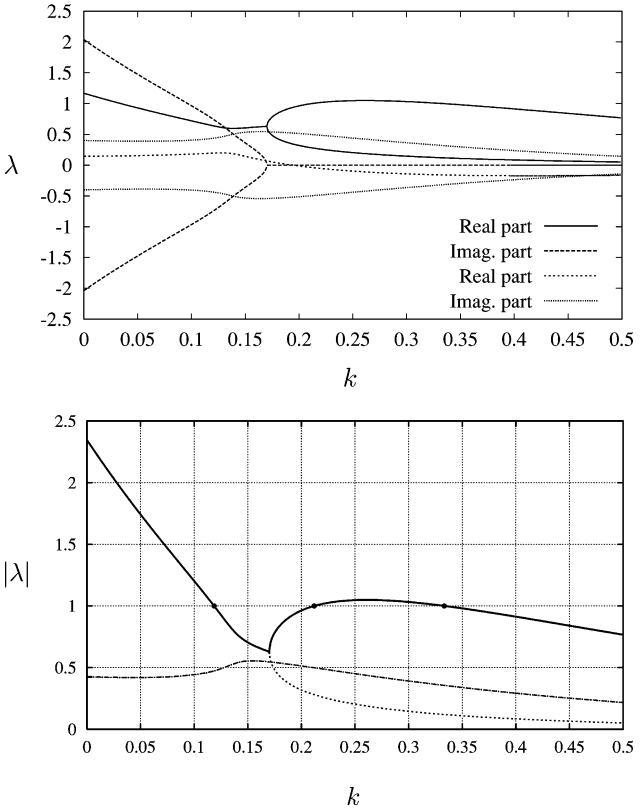

Fig. 13 Eigenvalues of the monodromy matrix and moduli vs k for $i = 40$ deg and $\varepsilon = 1.82$.

Keeping constant the value of k in Eq. (26), the following relation is obtained:

$$k^*(\varepsilon, i) = c$$

where c is the constant value of k, that is, $k = c$. This condition corresponds to a family of curves in the plane (ε, i), and c is the parameter of the family. (There is a curve for each value of c.) These curves also correspond to the stability boundary of the system, but now in the plane (ε, i). They divide the plane (ε, i) in two regions. In one of them the basic periodic solution is unstable, and in the other one is asymptotically stable. Obviously, on the boundary of the stability domain $|\lambda|_{\max} = 1$.

Figure 15 shows the boundary of the stability domain in the plane (ε, i) (curves $k = c$) for different values of k ($k = 1 \times 10^{-3}$, $2 \times 10^{-3}, \ldots, 10 \times 10^{-3}$). Note that the stable region shrinks, that is, ε decreases, when i increases, which is the expected behavior for this kind of model in which the value of ε is kept constant along the orbit. For a given curve, the value of ε reaches a minimum—maximum instability when $i \approx 55$ deg; the theory developed in Ref. 7 for small values of $\varepsilon \times \sin i$ predicts that the minimum is at $i = \arctan\sqrt{2} \approx 54.75$ deg.

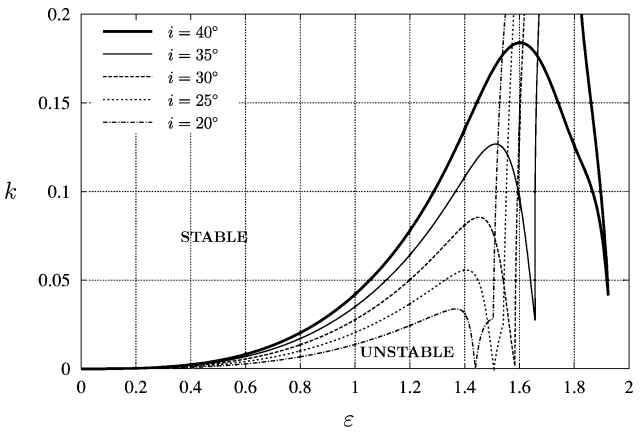

Fig. 14 Stability domain in the plane (ε, k) for different values of i.

Additional Comments About the Model

The analysis carried out in the preceding sections cannot be directly applied to a real tether. In fact, the analysis assumes a constant value for the parameter ε, which implies a constant torque produced by the electrodynamic forces about the system center of mass. However, the tether current depends on two distinct parameters: 1) the motional electric field E_m given by Eq. (7) and 2) the electronic plasma density of the ionosphere n_∞. For any inclined orbit, both parameters change along it, and, consequently, ε will also change along the orbit. Moreover, the tether librations affect the value of E_m, which decreases when the tether separates from the local vertical.

It would be possible to keep constant the value of ε for any kind of tether, bare or insulated. To do that, a variable resistor could be introduced in series with the tether, which would be used to keep constant the value of ε along the orbit. However, this technique is not completely practical because such a constant value would be very close to the minimum tether current (along the orbit), and the thruster performances of the tether would be seriously diminished. Moreover, the constant tether current assumption brings a drawback with it, that is, the effects of the electrodynamic forces acting on the tether could be overestimated.

However, the analysis of this paper opens the door to more specialized analysis for particular cases. For example, releasing the assumption of constant value for ε, we would reach a more accurate description of the electrodynamic forces acting on the system and, therefore, on the dynamic instability affecting electrodynamic tethers flying in inclined orbits. From this point of view, the release of this assumption should facilitate the stabilization of the tether librations. Because tether current depends closely on the device used to collect electrons and also on the operating regime, thruster or generator, the analysis must opt for a particular tether configuration.

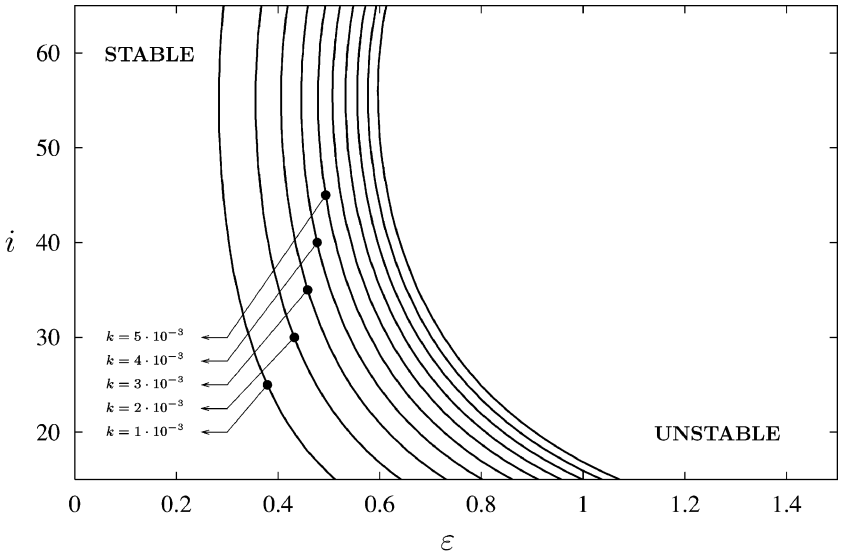

Fig. 15 Stability domain in the plane (ε, i) for different values of k.

For example, in Refs. 15 and 16 the bare tether has been analyzed in the long-tether regime of the generator mode. New free nondimensional parameters have been introduced in both papers to show how to reformulate the governing equations in order to take into account the dependence of the tether current on the actual tether position in the orbital frame and the variations along the orbit. In such a case, the parameter ε changes with the tether position and along the orbit. Using the same nontilted dipole model for the geomagnetic field, the papers show that there are also 2π-periodic solutions that are unstable without damping or control.

For an actual tether in Earth's orbit, however, the geomagnetic field is clearly much more complex than the one corresponding to an aligned dipole model. Forcing terms with a new period associated with the daily Earth rotation appear in the governing equations. As a consequence, the periodic solutions disappear for most orbits, and they only exist in some resonant cases. Moreover, the real tethers exhibit flexibility and elasticity, which introduce other temporal scales in the problem that contribute to destroying the periodicity. Finally, the evolution of the orbit of the system center of mass introduces additional perturbations in the problem. For example, any eccentricity would induce self-excited librations that reinforce the instability. Thus, in a real tether we will not have, in general, the periodic solutions that we consider in this paper. However, the periodic solutions that we found are important because they permit to asses the magnitude of the inherent dynamic instability affecting electrodynamic tethers flying in inclined orbits (without damping or control). Moreover, the effects that prevent the existence of periodic solutions can be considered as perturbations of the model that we present here. In such a case, it should be necessary to assess if those perturbations remove the asymptotic stable character from the periodic solution; such a stable character is the main consequence of the control scheme considered in this section.

Related to these matters, another question arises: the choice of the periodic orbit as the starting point of the operation in a given inclination i. For each value of ε, we have a periodic solution that tends to the equilibrium position along the local vertical when $\varepsilon \to 0$. The stabilization carried out by this control scheme requires to start the procedure close to the periodic orbit. To do that, it should be necessary to start from the natural equilibrium position of the tether along the local vertical and to increase the tether current progressively until reaching the desired value of ε. Note that to reach the periodic solution starting from the local vertical is easy for small values of ε because the periodic orbit is asymptotically stable and very close to the local vertical. Some problems would arise when the value of ε becomes of order unity, depending of the influence of the perturbing effect considered. These important points should be analyzed in the future.

Second Control Scheme

Recently, new control techniques have been developed related with chaos. Most of them try to convert chaotic behavior into a periodic or constant motion (for example, see Ref. 1). To use the basic periodic orbit as the starting point of the operation of the electrodynamic tether, some kind of device must be used to avoid the problems associated with its unstable character. In this paper we will check a control scheme, which is a natural extension of the TDAS that was used successfully in Ref. 5 to stabilize a gravity-gradient satellite in an elliptical orbit. The main innovation is that the scheme will be applied to a system with two degrees-of freedom.

However, some observations could be helpful in order to clarify a few points of the control problem that we face. First of all, the TDAS has been used to control chaotic motions that appear in several kinds of systems: autonomous, nonautonomous, self-excited, conservative, etc. In our case chaos is not the main concern because the more important characteristic of the physical problem is a nonlinear resonance that introduces energy into the system in a continuous way. We are dealing with a destabilizing mechanism, which is a bit different from the ones usually found in the literature.

In this section we assume that the tether is acted upon additional forces, which introduce new terms in the governing equations in order to control the tether dynamic in an effective way. For the moment, we avoid to describe what kind of device would be used to produce the additional forces, and we will assume that the control scheme leads to the following governing equations:

$$\ddot{\theta} - 2(1+\dot{\theta})\dot{\varphi}\tan\varphi + \tfrac{3}{2}\sin 2\theta = -\varepsilon \cdot [\sin i \tan\varphi h_1(\nu,\theta) + \cos i] - k_1[\dot{\theta}(\nu) - \dot{\theta}(\nu - 2\pi)] \tag{27}$$

$$\ddot{\varphi} + \sin\varphi\cos\varphi[(1+\dot{\theta})^2 + 3\cos^2\theta] = +\varepsilon \sin i \cdot h_2(\nu,\theta) - k_2[\dot{\varphi}(\nu) - \dot{\varphi}(\nu - 2\pi)] \tag{28}$$

The novelty is in the control terms $-k_1[\dot{\theta}(\nu) - \dot{\theta}(\nu - 2\pi)]$ and $-k_2[\dot{\varphi}(\nu) - \dot{\varphi}(\nu - 2\pi)]$ that provide the control mechanism that we would like to check. Both terms should control the growth of the oscillations of θ and φ as a result of the unstable dynamics. Because, they involve the nondimensional period of the basic periodic solution, 2π, when the system follows a 2π-periodic solution of Eqs. (11) and (12), both terms vanish. Thus, any 2π-periodic solution of the system (11) and (12) is also a 2π-periodic solution of the system (27) and (28).

If the control scheme were to be successful, the basic periodic solution of the noncontrolled problem (11) and (12) would become

asymptotically stable as periodic solution of the controlled system (27) and (28). In such a case, any orbit of the controlled system would approach the basic periodic solution when times goes on. Thus, after a while, the control terms becomes very small because they would tend to zero when $t \to \infty$. If from the very beginning the system is operated close to the basic periodic solution, it can be controlled with small controlling forces, an attractive feature of the control law.

Note that, if successful, the method has two important advantages related with the feedback used: it does not requires rapid switching or sampling, nor does it require a reference signal corresponding to the desired orbit.

Thus, the stability properties of the basic periodic solution as a trajectory of the controlled system (27) and (28) should be studied. One option is the Poincaré method of continuation of periodic orbits. [The procedure must be appropriately updated to take into account that Eqs. (27) and (28) involve delayed terms.] It can be implemented by taking anyone of the parameters k_1 or k_2 as the parameter of a family of periodic orbits embedding the basic periodic solution. However, two new functions must be introduced:

$$f(\nu) = \theta(\nu - 2\pi), \qquad g(\nu) = \varphi(\nu - 2\pi)$$

together with the equations for their time evolution, to be integrated from the following initial conditions:

$$f(\nu_0) = \theta(\nu_0 - 2\pi), \qquad \dot{f}(\nu_0) = \dot{\theta}(\nu_0 - 2\pi)$$

$$g(\nu_0) = \varphi(\nu_0 - 2\pi), \qquad \dot{g}(\nu_0) = \dot{\varphi}(\nu_0 - 2\pi)$$

Notice that all of these initial conditions becomes free parameters that should be added to the free parameters i, ε, k_1, and k_2 of the system. The number of free parameters turns out to be too large, and the Poincaré method of continuation of periodic orbits becomes almost useless. This is the weak point of this procedure.

TDAS Stability Analysis

To integrate the delayed equations (27) and (28) from the initial conditions (14) at $\nu = \nu_0$, the functions $\theta(\nu)$ and $\varphi(\nu)$ must be given in the previous period $[\nu_0 - 2\pi, \nu_0]$. From the point of view of the operation of the tether, these functions can be obtained by integrating Eqs. (27) and (28) from the initial conditions (14), but for negative times, with $\varepsilon = 0$, $k_1 = k_2 = 0$. Remember that $t = 0$, the initial time, is the moment when the tether is turned on.

A second option is to carry out the stability analysis of the basic periodic solution as trajectory of Eqs. (27) and (28), following the theory developed in Ref. 4. However, before undertaking such a cumbersome analysis we made some tests in order to get some feeling on the system behavior. Unfortunately the tests gave us a negative answer about the stability of the periodic orbit.

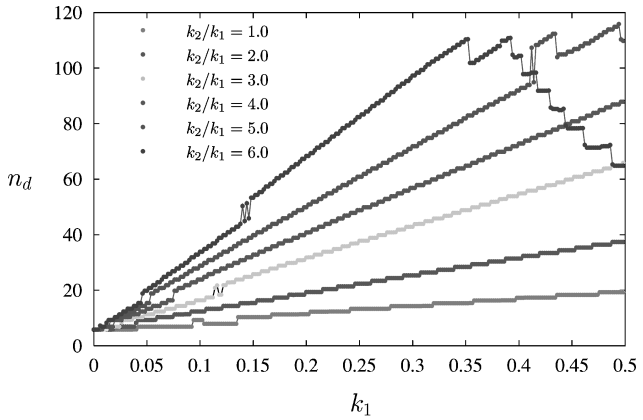

Fig. 16 Number of orbits spent to double the initial energy vs k_1 for different values of the ratio k_2/k_1. Here, $\varepsilon = 1.5$ and $i = 40$ deg. Lowest curve for $k_2/k_1 = 1$.

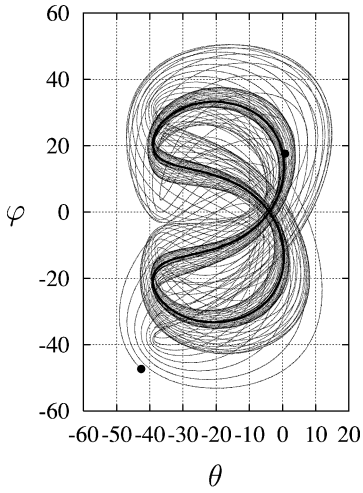

Fig. 17 Destabilized orbit until reach twice energy. Here, $\varepsilon = 1.5$, and $i = 40$ deg.

Figure 4 shows an unstable periodic orbit corresponding to $\varepsilon = 1.5$ and $i = 40$ deg. This orbit was selected for the tests. Equations (27) and (28) were integrated starting from the initial conditions (24) and (25) with $\eta_1 = 0.01$ and $\eta_2 = 0.01$, for different combinations of the control parameters k_1 and k_2. We expected to find stable behavior for values of k_1 and k_2 beyond some critical threshold. But in all cases, when time goes on, the trajectory moved away from the periodic solution after some time.

Along the destabilization process, the total energy of the system as given by Eq. (17) is increasing gradually. Figure 16, which summarizes the results of our tests, shows the time (in orbital periods) spent to double the initial energy of the system, as a function of k_1, for different values of the ratio $k_2/k_1 = 1, 2, 3, 4, 5$, and 6.

Figure 16 shows clearly that for increasing values of the control parameter it takes more time to double the energy and, therefore, to destabilize the system. However, the linear growth of that time is a clear sign of unstable character. In fact, in all of our calculations the orbit reached the transition from libration to rotation after several orbital periods.

Figure 17 shows a typical evolution of the trajectory. In this case the control parameters take the values: $k_1 = 0.204$ and $k_2 = 1.224$. The final position corresponds to the point where the total energy doubles its initial value, for the first time. The orbit shown in this figure spent many orbits in the neighborhoods of the periodic orbit, but from the very beginning it moves away from it. When it reaches a value of twice energy, the phase-space trajectory is far away from the periodic orbit.

The reason why TDAS fails to stabilize the orbit must be found in the energy flow to the system coming from the electrodynamic forces. Similar behavior has been detected in forced system. For example, in Ref. 4 the authors mention an example of a forced pendulum where TDAS also failed.

Conclusions

Electrodynamic tethers exhibit a dynamic instability. As a consequence, the amplitude of the tether libration grow gradually and destabilize the system. To avoid such destabilization process, some kind of damping or control must be introduced in the system.

Using a very simple model to describe the system dynamics, we analyze in this paper two control laws with the aim of clarifying if they are appropriate to stabilize the system.

In the first control law we take an unstable periodic trajectory of the phase space as reference orbit, and we introduce damping forces on the system, which depend on the difference between the real orbit and the reference orbit. We show that for equal values of the two control parameters the system can be stabilized when the control parameter is greater than a threshold value, which depends on the orbital inclination and the strength of the electrodynamic forces.

This control law has advantages and drawbacks. On the advantages side we have to mention the following:

1) It converts the reference orbit (an unstable periodic orbit of the uncontrolled system) in an asymptotically stable orbit of the controlled system.

2) Because of this asymptotically stable character, the forces needed to control the system become small when time progresses. If the tether starts its motion close to the reference orbit, then it can be readily controlled.

3) It can be extended without significant difficulties to more realist models (bare tethers with variable current, for example). In some cases, a close structure has been found[15,16] with periodic orbits that could, likely, be stabilized with the same strategy (obviously, with a different reference orbit).

On the drawbacks side, we should mention the following:

1) To use a reference orbit could be a problem because for the real operation of the tether it is necessary to estimate the reference orbit appropriately. Any mistake in the selection of the reference orbit introduces an unknown excitation on the system, which will be forced to follows a nonnatural orbit that involves a greater control effort.

2) There is no immediate way to introduce the forces needed in the control process on the system. This point must be analyzed in detail before implementing this procedure. However, we believe that those forces could be produced by a movable boom at the tether attachment point.

3) In a real case, the orbit of the mother spacecraft is changing continually. This force to change the reference orbit appropriately, and this adjusting process could introduce instabilities in the system.

The second control law is an extension of the time-delayed autosynchronization (TDAS) method to a dynamical system with two degrees of freedom. This king of control schemes has been used in some situations involving orbital and attitude dynamics of a spacecraft, for a one-degree-of-freedom system.[5] If successful, the method has two important advantages related with the feedback used: it does not requires rapid switching or sampling, nor does it require a reference signal corresponding to the desired orbit.

Unfortunately, the TDAS control scheme does not work appropriately in the problem of the electrodynamic tethers. Our calculations show that this control law delays the instability, but it does not stabilize the unstable periodic orbit for reasonable values of the control parameters.

A possibility to stabilize the tether with this kind of techniques is to use the extended time-delayed autosynchronization (ETDAS) method, which is an extension of the TDAS method. The ETDAS has been used with success in some cases where TDAS failed.[3,4]

There are some natural continuations of this work: 1) to check the ETDAS procedure and 2) to analyze if a movable boom can provide the control forces needed to stabilize the system with the second control law.

Acknowledgments

The work of J. Peláez was carried out in the framework of the research project entitled “Estabilidad y Simulación Dinámica de Tethers” (BFM2001-3663), supported by the Dirección General de Investigación of the Spanish Ministry of Science and Technology. Part of the work of J. Peláez was done during a visit at the Smithsonain Astrophysical Observatory (SAO) in the Summer of 2002. J. Peláez thanks SAO for the support provided.

References

[1]Pyragas, K., “Control of Chaos via Extended Delay Feedback,” *Physics Letters A*, Vol. 206, Oct. 1995, pp. 323–330.

[2]Pyragas, K., “Continuous Control of Chaos by Self-Controlling Feedback,” *Physics Letters A*, Vol. 170, No. 6, 1992, pp. 421–428.

[3]Socolar, J. E. S., Sukow, D. W., and Gauthier, D. J., “Stabilizing Unstable Periodic Orbits in Fast Dynamical Systems,” *Physics Review E*, Vol. 50, No. 4, 1994, pp. 3245–3248.

[4]Bleich, M. E., and Socolar, J. E. S., “Stability of Periodic Orbits Controlled by Time-Delay Feedback,” *Physics Letters A*, Vol. 210, Jan. 1996, pp. 87–94.

[5]Fujii, H. A., Ichiki, W., Suda, S., and Watanabe, T. R., “Chaos Analysis on Librational Control of Gravity-Gradient Satellite in Elliptic Orbit,” *Journal of Guidance, Control, and Dynamics*, Vol. 23, No. 1, 2000, pp. 145, 146.

[6]Peláez, J., Lorenzini, E. C., López-Rebollal, O., and Ruiz, M., “A New Kind of Dynamic Instability in Electrodynamic Tethers,” *Advances in the Astronautical Sciences*, Vol. 105, Pt. 2, 2000, pp. 1367–1386.

[7]Peláez, J., Lorenzini, E. C., López-Rebollal, O., and Ruiz, M., “A New Kind of Dynamic Instability in Electrodynamic Tethers,” *Journal of the Astronautical Sciences*, Vol. 48, No. 4, 2000, pp. 449–476.

[8]Peláez, J., Ruiz, M., López-Rebollal, O., Lorenzini, E. C., and Cosmo, M. L., “A Two Bar Model for the Dynamics and Stability of Electrodynamic Tethers,” *Journal of Guidance, Control, and Dynamics*, Vol. 25, No. 6, 2002, pp. 1125–1135.

[9]Peláez, J., and Lara, M., “Periodic Solutions in Rigid Electrodynamic Tethers on Inclined Orbits,” *Advances in the Astronautical Sciences*, Vol. 108, Pt. 2, 2001, pp. 1189–1208.

[10]Peláez, J., and Lara, M., “Periodic Solutions in Electrodynamic Tethers on Inclined Orbits,” *Journal of Guidance, Control, and Dynamics*, Vol. 26, No. 3, 2003, pp. 395–406.

[11]Dobrowolny, M., “Lateral Oscillations of an Electrodynamic Tether,” *Journal of the Astronautical Sciences*, Vol. 50, No. 2, 2002, pp. 125–147.

[12]Corsi, J., and Iess, L., “Stability and Control of Electrodynamic Tethers for De-Orbiting Applications,” *Acta Astronautica*, Vol. 48, No. 5–12, 2001, pp. 491–501.

[13]Somenzi, L., Iess, L., and Peláez, J., “Linear Stability Analysis of Flexible Electrodynamic Tethers,” *Advances in the Astronautical Sciences*, Vol. 116, Pt. 1, 2004, pp. 615–634.

[14]Lara, M., and Peláez, J., “On the Numerical Continuation of Periodic Orbits: An Intrinsic, 3-Dimensional, Differential, Predictor-Corrector Algorithm,” *Astronomy and Astrophysics*, Vol. 389, No. 2, 2002, pp. 692–701.

[15]Peláez, J., López-Rebollal, O., Lara, M., and Ahedo, E., “Dynamic Stability of a Bare Tether as a Deorbiting Device,” *Advances in the Astronautical Sciences*, Vol. 112, Pt. 2, 2002, pp. 1257–1274.

[16]Peláez, J., and Lara, M., “Damping in the Dynamic Stability of Deorbiting Bare Tethers,” *Advances in the Astronautical Sciences*, Vol. 114, Pt. 3, 2003, pp. 1647–1666.